Langmuir

Letter

pubs.acs.org/Langmuir

Porous Polymer Nanostructures Fabricated by the Surface-Induced Phase Separation of Polymer Solutions in Anodic Aluminum Oxide Templates

Tzu-Hui Wei, Mu-Huan Chi, Chia-Chan Tsai, Hao-Wen Ko, and Jiun-Tai Chen*

Department of Applied Chemistry, National Chiao Tung University, Hsinchu, Taiwan 30050

Supporting Information

ABSTRACT: We study the formation of porous polymer nanostructures fabricated by the surface-induced phase separation of polymer solutions in anodic aluminum oxide (AAO) templates. Poly(methyl methacrylate) (PMMA) and tetrahydrofuran (THF) are used to investigate the evolution process of the surface-induced phase separation. With the longer immersion time of the AAO template in the polymer solution, the size of the solvent-rich droplet is increased by the coarsening process, resulting in the formation of porous polymer nanostructures. The coarsening mechanism is further evaluated by changing the experimental parameters including the immersion time, the polymer concentration, the polymer molecular weight, and the solvent quality. Under conditions in which polymer solutions have higher viscosities, the coarsening process is slowed down and the formation of the porous nanostructures is prohibited. The prevention of the porous nanostructures can also be realized by adding water to the PMMA/THF solution before the immersion process.

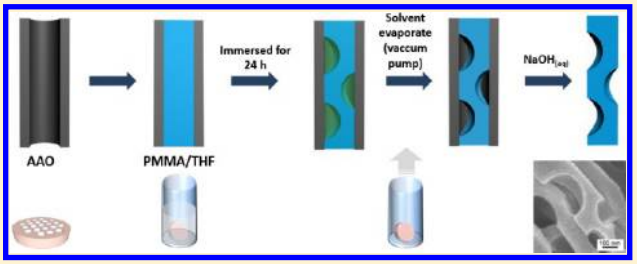

INTRODUCTION

In recent years, 1D polymer nanostructures have attracted a great amount of attention because of their applications in different fields such as biosensors, drug delivery, and organic solar cells.[1−4] One of the most widely used methods of preparing 1D polymer nanostructures is the template method because of its simplicity and versatility.[5−8] In the template method, the template is used as a scaffold, and polymers are shaped by the geometry of the template. A commonly used template is the anodic aluminum oxide (AAO) template, which is produced by electrochemical anodization from aluminum. The AAO template contains cylindrical channels, and the sizes of the channels can be controlled by the anodization conditions.[9,10]

There are three major approaches to preparing polymer nanostructures using templates, including the melt method, the solvent annealing method, and the solution method.[11] In the melt method, polymer chains wet the templates after being annealed above the glass-transition temperatures or the melting temperatures of the polymers.[11−16] In the solvent annealing method, polymers chains wet the templates while being annealed in different solvent vapors.[17,18] In the solution method, polymers are dissolved in a suitable solvent and infiltrate the channels of the template by capillary force.[19] Polymer nanostructures are obtained after the extraction or evaporation of the solvent.

Although different polymer nanostructures can be prepared by using these template-based approaches, the relationship between the preparation condition and the resultant morphology of the polymer nanostructures has not been fully understood, especially when the polymers infiltrate the channels of the template as solutions. Polymer nanotubes are usually obtained using the solution template wetting method because of the adsorption of the polymer chains on the channel walls of the template. The thickness of the polymer nanotubes can also be controlled simply by varying the polymer concentration.

Using polystyrene (PS) solutions, Wendorff et al. studied the effect of molecular weight on the formation of polystyrene (PS) nanostructures in AAO templates.[20] PS nanowires, nanotubes, or cylindrical structures with regular voids were prepared by varying the molecular weight of the polymers. Later, Feng and Jin demonstrated that the different interfacial affinities of polymer and solvent for alumina can influence the morphologies of polymer nanostructures.[21] PS nanospheres, nanocapsules, or nanorods can be obtained by using electron-pair donor solvents. More recently, we studied the effect of a nonsolvent on the formation of polymer nanostructures. Water (nonsolvent) was added to the polymer solution confined in the channels of AAO templates, resulting in the formation of polymer nanospheres or nanorods.[15]

Despite previous work, the effects of many interrelating factors on the formation of polymer nanostructures using the solution template wetting method are still unclear and need to be investigated further. In this work, we demonstrate a systematic study to control the formation of porous polymer nanostructures using AAO templates. For the polymer/solvent system, we use poly(methyl methacrylate) (PMMA) and

Received: May 13, 2013
Revised: July 23, 2013
Published: July 23, 2013

   dx.doi.org/10.1021/la401797f | *Langmuir* 2013, 29, 9972−9978

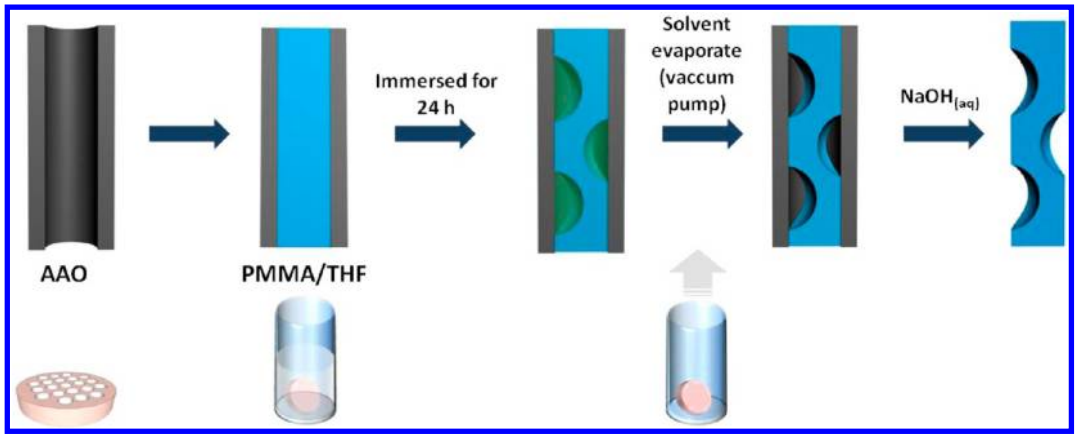

Figure 1. Schematic illustration of the experimental process used to fabricate porous polymer nanostructures using the AAO template. The AAO template is immersed in the PMMA/THF solution for 24 h, and porous polymer nanostructures are obtained after solvent evaporation by a vacuum pump. The template is selectively removed by a 5 wt % NaOH solution.

tetrahydrofuran (THF) as the model materials, which have similar affinities for the alumina wall.

Surface-induced phase separation of the PMMA/THF solution is involved in the formation process of the 1D porous nanostructures. At first, small solvent-rich droplets are formed at the interface between the solution and the alumina wall, initiated by the surface-induced nucleation or spinodal decomposition. The size of the solvent-rich droplet is increased by a coarsening process, which is caused by three possible mechanisms: Ostwald ripening, coalescence, and hydrodynamic flow.[22] Therefore, as the immersion time of the AAO template in the polymer solution increases, the size of the solvent-rich droplet increases, resulting in the formation of porous polymer nanostructures after the evaporation of the solvent.

The phase separation of polymer solution is examined by changing different experimental parameters, including the immersion time, the polymer concentration, and the polymer molecular weight. It is also found that the formation of the porous nanostructures can be prohibited by adding water to the polymer solution. In the past, controlling the phase separation of polymer solution was a versatile method for developing microporous polymer membranes that can be used for applications such as filtration, reverse osmosis, and gas separation.[22] The concept of studying the phase separation of polymer solution in cylindrical channels, as we demonstrate here, further provides a unique way to prepare 1D porous polymer nanostructures that are useful for developing new membrane applications.

EXPERIMENTAL SECTION

Materials. Poly(methyl methacrylate) (PMMA) with weight-average molecular weights (M_w) of 47 (PDI = 1.3), 97 (PDI = 2.1), 183 (PDI = 1.7), and 910 (PDI = 1.3) kg/mol were purchased from Sigma-Aldrich and Polymer Source Inc. Anhydrous tetrahydrofuran (THF) was obtained from Tedia. Acetone and toluene were purchased from Echo Chemical. Anodic aluminum oxides (AAO) templates (pore diameter ~150–400 nm, thickness ~60 μm) were obtained from Whatman. Polycarbonate filters (VCTP, pore size ~0.1 μm) were purchased from Millipore. Sodium hydroxide (NaOH) was obtained from TEDIA.

Fabrication of Porous PMMA Nanostructures. To make porous PMMA nanostructures, polymer solutions (PMMA in THF) of different concentrations (5, 10, 20, and 30 wt %) were first prepared. The AAO templates were immersed in the PMMA solutions for different lengths of time. After the templates were taken out of the polymer solutions with tweezers, the residual solution outside the channels of the AAO templates was removed by wiping with Kimwipes. The samples were then dried with a vacuum pump to remove the solvent and immersed in 5 wt % NaOH(aq) to dissolve the AAO templates selectively. Finally, the samples were washed and filtered with deionized water using polycarbonate filters (0.1 μm).

For the preparation of water-containing polymer solutions, 15 mL of a 5 wt % PMMA/THF solution was first made. The PMMA solution was then distributed into several sample bottles (2 mL). Subsequently, different amounts of deionized water were added to the sample bottles with a 200 μL pipet, and 8, 26, 31, 39, and 64 wt % (water/solution) water-containing PMMA solutions were prepared. Similar immersion procedures were performed for the water-containing PMMA solutions.

Structure Analysis and Characterization. After the fabrication of the polymer nanostructures, the samples were characterized by a JEOL JSM-7401 model scanning electron microscope (SEM) at an accelerating voltage of 5 kV. The samples were dried in a vacuum oven and coated with ~4 nm of platinum before the SEM measurement. To measure the cross-sectional views of the channels of the AAO templates, the samples were prepared by breaking the AAO templates using a razor blade. The polymer samples were also characterized with a JEOL JEM-2100 transmission electron microscope (TEM) with an acceleration voltage of 200 kV. The samples were placed onto copper grids coated with Formvar or carbon before the TEM measurement.

RESULTS AND DISCUSSION

In this work, AAO templates are used to study the phase separation of polymer solutions. AAO templates are widely used because of their regular pore distributions and high aspect ratios of cylindrical channels. The top views and cross-sectional views of the SEM images of the AAO templates are shown in the Supporting Information. The average size of the cylindrical channels is ~240 nm. Although some channel ends are not circular from the top views of the AAO templates, the cross-sectional views demonstrate that most of the channels are straight and the wall surfaces of the channels are smooth.

The schematic illustration of the experimental process used to fabricate the porous polymer nanostructures is depicted in Figure 1. Poly(methyl methacrylate) (PMMA) and tetrahydrofuran (THF) that have similar affinities for the alumina wall are used as the model materials. After the preparation of the PMMA solution, the AAO template is immersed in the solution for different lengths of time. The PMMA solution wets the channels of the template by capillary force. According to Jurin's law, the height that the PMMA solution can reach is inversely

dx.doi.org/10.1021/la401797f | Langmuir 2013, 29, 9972–9978

proportional to the radius of the channels, as given by the following equation:[15]

$$h = \frac{2\gamma \cos\theta}{\rho g r} \quad (1)$$

where h is the maximum height, ρ is the density of the solution, g is gravity, r is the radius of the channel, γ is the surface tension of the solution, and θ is the contact angle of the solution meniscus at the channel wall. Because of the small channel diameters (~150−400 nm) of the AAO template, the maximum height that the polymer can reach is higher than the length of the cylindrical channels (~60 μm). The polymer solution can fill the channels within a second for dilute polymer solutions. After different lengths of immersion time, the samples are dried with a vacuum pump to remove the solvent. Subsequently, the polymer nanostructures can be released by selectively removing the AAO template using a 5 wt % NaOH solution.

Normally, the phase separation of polymer solutions is induced by thermal quenching.[22] In this study, surface-induced phase separation occurs in the cylindrical channels of the AAO templates during the immersion process. Solvent-rich droplets are formed on the channel walls of the AAO template because of the hydrogen bonding between the solvent (THF) and alumina. Later, the size of the solvent-rich droplets increases by a coarsening process. After the evaporation of the solvent, PMMA nanostructures with nanopores are formed.

The coarsening process is caused by three possible mechanisms, including Ostwald ripening, coalescence, and hydrodynamic flow. Ostwald ripening was first reported by Wilhelm Ostwald in 1896 and can be used to study the phase separation of polymer solutions.[23] The driving force of the Ostwald ripening in polymer solutions is to lower the interfacial energy between the solvent-rich and the polymer-rich phases. The molecules of small droplets of the dispersed phase dissolve because of higher curvatures and precipitate on the surfaces of large droplets. The total interfacial area of the different phases decreases, resulting in a decrease in the interfacial energy.[24] The domain sizes followed an asymptotic power-law relation

$$d \approx (D\xi)^{1/3} t^{1/3} \quad (2)$$

where d is the domain size, D is the diffusion constant, ξ is the correlation length, and t is the coarsening time.[25]

For the coalescence mechanism, coarsening is caused by two droplets impinging by translational diffusion, and a single droplet is formed. The coalescence mechanism is diffusion controlled, and the domain growth has a power-law relation with time

$$d \approx \left(\frac{k_B T}{\eta}\right)^{1/3} t^{1/3} \quad (3)$$

where k_B is the Boltzmann constant, T is the temperature, and η is the viscosity.[26] It has to be noted that both the Ostwald ripening and coalescence mechanisms have similar power law relationships with time ($d \approx t^{1/3}$).

The third coarsening mechanism is hydrodynamic flow. For the cylindrical part of a bicontinuous structure, the flow of inner fluid from a narrow to a wide region is induced by the gradient of pressure along the axis of the cylinder.[24] Inside the channels of the AAO templates, the bicontinuous solvent-rich and solvent-poor phases may be formed during the phase-separation process and the hydrodynamic flow can be induced. The domain growth is linear with time

$$d \approx \frac{\sigma}{\eta} t \quad (4)$$

where σ is the surface tension.[25]

Figure 2 shows a typical example of the porous PMMA nanostructures. The AAO templates are immersed in 5 wt % PMMA (M_w = 97 kg/mol)/THF solutions for 24 h, followed by the evaporation of THF using a vacuum pump. Figure 2a,b shows SEM images at low and high magnifications, respectively. Nanopores can be observed along the 1D polymer nanostructures. To confirm the porous PMMA nanostructures, TEM is performed. Figure 2c,d shows TEM images of the nanostructures at low and high magnifications, respectively. The sizes of the nanopores shown in the TEM images agree well with those observed by SEM.

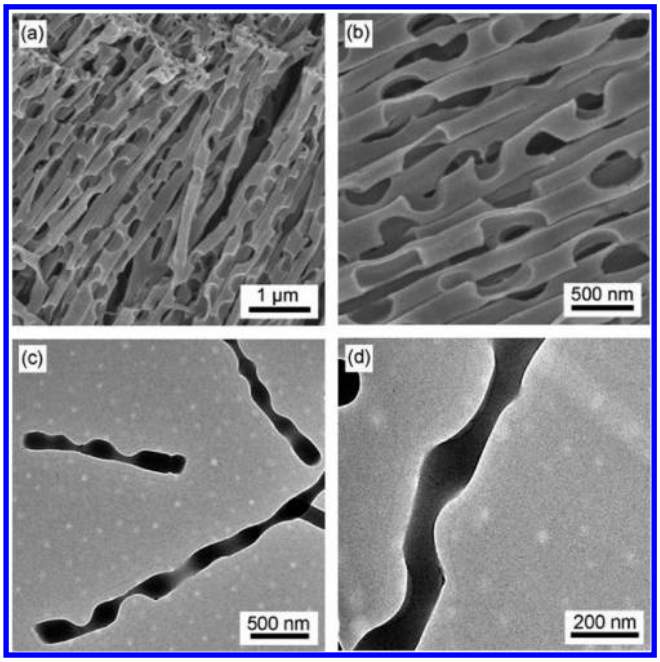

Figure 2. SEM and TEM images of porous PMMA (M_w = 97 kg/mol) nanostructures from 5 wt % PMMA/THF solutions. The AAO templates are immersed in the PMMA solutions for 24 h before the evaporation of the solvent. (a, b) SEM images at low and high magnification. (c, d) TEM images at low and high magnification.

According to the coarsening model, the immersion time of the AAO templates in the polymer solutions is critical to the formation of the porous PMMA nanostructures. With longer immersion times, the sizes of the solvent droplets increase, and the nanopores become larger in size. Figure 3 shows the PMMA (M_w = 97 kg/mol) nanostructures by immersing the AAO templates in 5 wt % PMMA/THF solutions for different lengths of time, from 10 s to 72 h. When the AAO template is immersed in the PMMA/THF solution for a very short time (a few seconds), only very small THF droplets are formed on the channel walls, caused by the substrate-induced nucleation. Therefore, the porous nanostructures are not apparent. Figure 3a shows the PMMA nanostructures when the AAO templates are immersed in the 5 wt % PMMA/THF solution for only 10 s, in which PMMA nanostructures with smooth or slightly curved surfaces are obtained.

dx.doi.org/10.1021/la401797f | Langmuir 2013, 29, 9972−9978

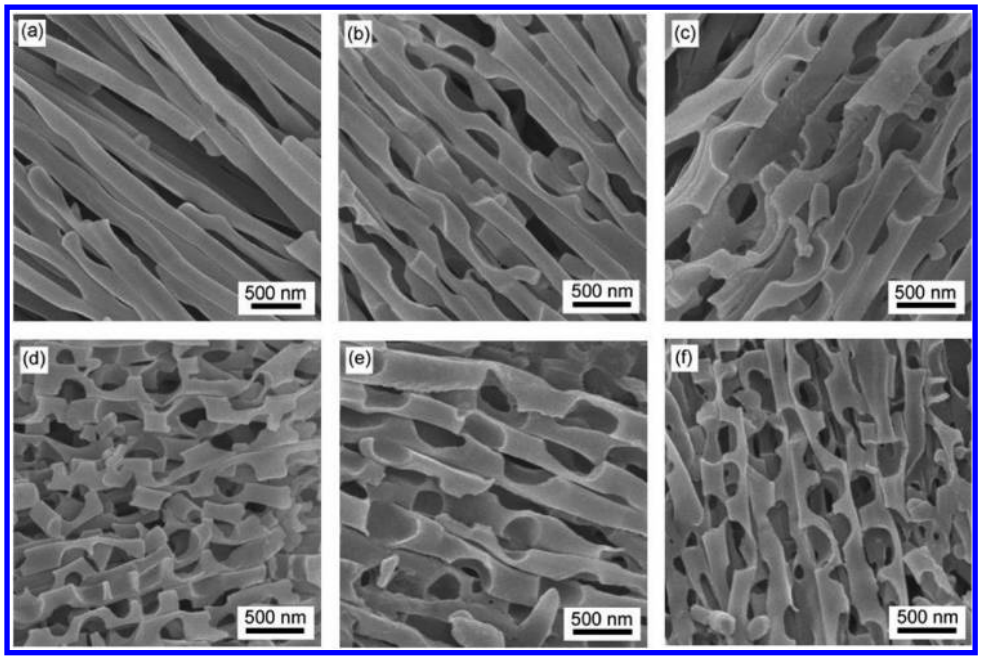

Figure 3. SEM images of porous PMMA (M_w = 97 kg/mol) nanostructures from 5 wt % PMMA/THF solutions. The AAO templates are immersed in the PMMA solutions for different lengths of time before the evaporation of the solvent: (a) 10 s, (b) 1 h, (c) 6 h, (d) 12 h, (e) 24 h, and (f) 72 h.

When the immersion time is increased to 1 h, the sizes of the solvent-rich droplets are larger, resulting in the formation of PMMA nanostructures with larger nanopores, as shown in Figure 3b. The trend in the increasing size of the nanopores is maintained as the immersion time is further increased to 6 and 12 h (Figure 3c,d). Finally, the sizes of the nanopores reach a maximum value with even longer immersion times (24 and 72 h), as shown in Figure 3e,f, respectively. In addition, TEM measurements are performed for the PMMA nanostructures obtained at different immersion times. The TEM results also confirm that the nanopores become larger in size with the immersion time, as shown in the Supporting Information.

To understand the phase separation and pore formation processes further, we also perform quantitative studies of the polymer samples. The relationship between the contact angles (θ_c) of the nanopores and the immersion time is investigated. The contact angles between the nanopores and the walls of the AAO surface are indicated in Figure 4a,b. The contact angles increase from ~25° at an immersion time of 10 s to ~75° at an immersion time of 12 h, as shown in Figure 4c. The contact angles remain at ~75° when the immersion times are increased up to 72 h. The angle measurements also confirm the coarsening model about the solvent-rich droplets and the formation of the porous polymer nanostructures. On the basis of the results of SEM, TEM, and contact angle measurements, the coarsening processes of the solvent-rich droplets at different immersion times are illustrated in Figure 4d. It has to be noted that the sizes of the nanopores do not equal to the sizes of the solvent-rich droplets before solvent evaporation, but the sizes of the solvent-rich droplets can still be largely represented by the size of the nanopores, assuming fast solvent evaporation. It is difficult to perform a quantitative analysis on the 3D features of the nanopores from the electron microscopy images. The quantitative surface and spatial analysis may be performed by using special software such as Mex 3D (Alicona Imaging GmbH). When this software is used, SEM images taken at different tilt angles can be mathematically processed and 3D SEM images can be reconstructed.

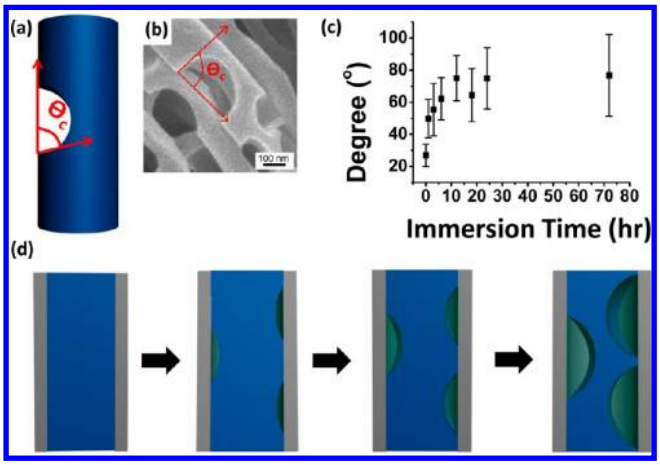

Figure 4. (a, b) Model and SEM image of the porous PMMA nanostructures. The contact angle (θ_c) of the pores is indicated in the graph. (c) Plot of the contact angle (θ_c) of the pores on the PMMA nanostructures versus the immersion time of AAO templates. (d) Graphical illustrations of the coarsening process of the solvent-rich droplets and the formation of the porous PMMA nanostructures.

In this work, PMMA/THF is used as the model system because PMMA and THF have similar affinities for the walls of the AAO templates. It is known that the AAO template has hydroxyl groups on the alumina surface. PMMA has oxygen with lone pair electrons, so hydrogen bonding is formed between the oxygen atoms of PMMA and the hydroxyl groups of the channel wall. THF is an electron-pair donor (EPD) solvent and has oxygen with lone pair electrons. Therefore, hydrogen bonds can also be formed between the oxygen atoms of THF and the hydroxyl groups of the alumina wall. Other EPD solvents, such as acetone, can also have effects. For example, porous PMMA nanostructures can be obtained from the PMMA/acetone solution. The SEM and TEM images of

dx.doi.org/10.1021/la401797f | *Langmuir* 2013, 29, 9972−9978

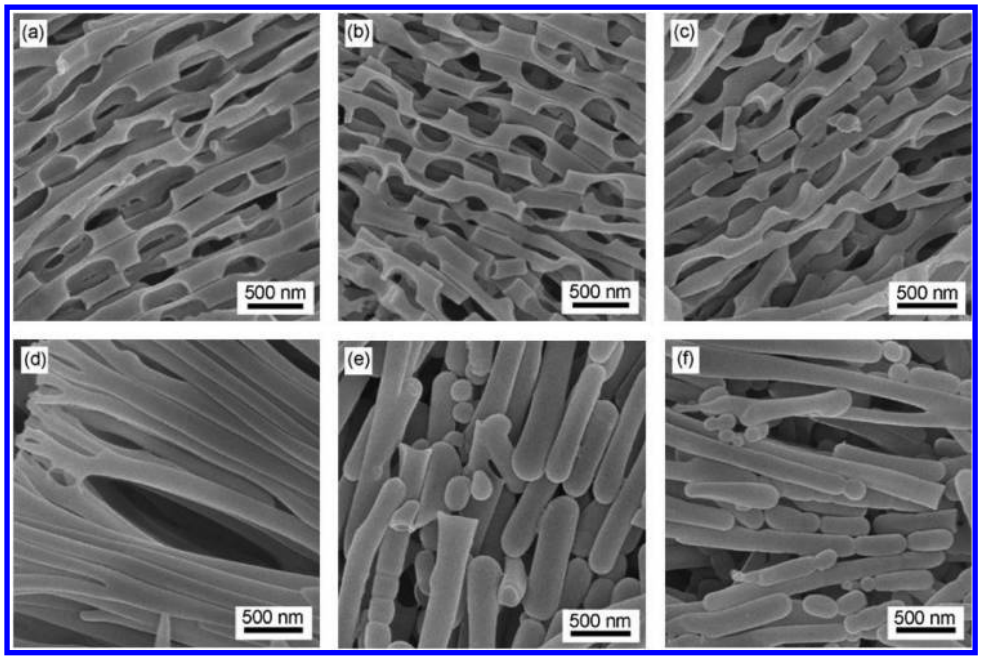

Figure 5. SEM images of PMMA (M_w = 97 kg/mol) nanostructures from water-containing PMMA/THF solutions. Different amounts of water are added to 5 wt % PMMA/solution in ratios of (a) 0, (b) 8, (c) 26, (d) 31, (e) 39, and (f) 64 wt % (water/solution). The immersion times of AAO templates in the polymer solutions are all 24 h.

porous PMMA (M_w = 97 kg/mol) nanostructures obtained by immersing the AAO templates in PMMA/acetone solutions for 10 s and for 24 h are shown in the Supporting Information.

When the polymer has a much stronger affinity for the AAO walls than does the solvent, phase separation of the polymer solution does not occur. Therefore, polymer nanostructures with smooth surfaces are obtained when PMMA is dissolved in other solvents such as toluene, DMF, chloroform, and benzene. For example, PMMA (M_w = 97 kg/mol) nanostructures with smooth surfaces are obtained by immersing an AAO template in a 5 wt % PMMA/toluene solution, as shown in the Supporting Information.

When the solvent has a much stronger affinity for the AAO walls than does the polymer, a depletion layer of solvent on the alumina wall is formed. Feng and Jin studied the formation of a depletion layer of THF on the channel walls of the AAO templates when a solution of polystyrene/THF was used.[21] They found that polystyrene nanospheres and nanorods instead of nanotubes can be obtained.

For the thermally induced phase separation of polymer solutions, gravity plays an important role in a later stage of the coarsening process, and macroscopic layers are formed.[22] To extend the time scales for studying the coarsening in the absence of macroscopic phase separation resulting from gravitational effects, isopycnic polymer−solvent systems have been used where the densities of polymer and solvent are nearly matched.[27] For example, Song and Torkelson used PS-diethyl malonate as the isopycnic polymer−solvent system to investigate the coarsening process of polymer solutions.[24] In this study, however, the gravity-induced coarsening is ignored because the size scale in the AAO channels is much smaller than the capillary length.[22]

The effect of polymer concentration on the phase separation of polymer solution and the formation of porous PMMA nanostructures is also investigated. Figure S5a−d shows SEM images of PMMA (M_w = 97 kg/mol) nanostructures by immersing the AAO templates in 5, 10, 20, and 30 wt % PMMA/THF solutions for 24 h. Fragmented PMMA nanostructures are observed when the concentration of polymer solution is low, such as 1 wt %. Porous PMMA nanostructures are obtained when the polymer concentration is increased to 5 wt %, as shown in Figure S5a. In Figure S5b, the polymer concentration is further increased to 10 wt %, and porous structures are still observed. However, the porous structures are not formed when the concentration is increased to 20 and 30 wt %, as shown in Figures S5c and S5d, respectively. Only polymer nanostructures with smooth surfaces are obtained. Therefore, the phase separation of the polymer solution in cylindrical channels is also affected by the concentration of the polymer solution. The absence of the porous nanostructures is attributed to the higher viscosity of the polymer solutions with higher concentrations that can decrease the diffusion rate of the polymer and the solvent molecules.

The molecular weights of the polymers are also important in controlling the phase-separation process. SEM images of PMMA nanostructures from 5 wt % PMMA/THF solution with weight-average molecular weights of 47, 97, 183, and 910 kg/mol are shown in Figure S6, and the immersion times are all 24 h. Porous PMMA nanostructures are obtained for polymers with molecular weights of 47 and 97 kg/mol, and porous nanostructures are not observed when the molecular weights are 183 and 910 kg/mol. These results agree with those obtained by changing the polymer concentrations. Similar to the effect of increasing the polymer concentration, increasing the polymer molecular weight can increase the viscosity of the polymer solution, resulting in the delay or inhibition of phase separation of the polymer solutions in the cylindrical channels.

To study the effect of solvent quality in the polymer solution, different amounts of deionized water are intentionally added to the polymer solutions. Water is soluble in THF and can be easily mixed with the PMMA/THF solution. Figure 5 shows

dx.doi.org/10.1021/la401797f | *Langmuir* 2013, 29, 9972−9978

SEM images of the PMMA (M_w = 97 kg/mol) nanostructures by immersing the AAO templates in 2 mL of 5 wt % PMMA/THF solutions that contain different amounts of deionized water. Porous PMMA nanostructures are observed from a polymer solution that contains no deionized water, as shown in Figure 5a. The nanopores are still observed using an 8 wt % (water/solution) solution (Figure 5b), but when the amount of deionized water is increased to 26 wt % (water/solution), the shape of the nanopores starts to change, as shown in Figure 5c. When the water content is further increased to 31 wt %, pores are not observed (Figure 5d). In addition to the disappearance of the pores, nanospheres or round-shaped nanorods are formed with further increases in the amount of deionized water in the polymer solutions, as shown in Figure 5e,f. Therefore, adding a nonsolvent such as water can prohibit the formation of porous nanostructures because depletion layers of water are formed at the interface of the solution and the alumina wall.

CONCLUSIONS

We studied the formation of porous PMMA nanostructures using AAO templates. PMMA and THF have similar affinities for the alumna wall and are used as model materials. Once the AAO template is immersed in the PMMA/THF solution, the cylindrical channels are infiltrated with solution via capillary force. Small droplets of solvent-rich phases are formed at the interface between the polymer solution and the alumina wall, as initiated by surface-induced nucleation or spinodal decomposition. For the longer immersion time of the AAO template in the polymer solution, the size of the solvent-rich droplet increases by the coarsening process through the mechanisms of Ostwald ripening, coalescence, and hydrodynamic flow. After the evaporation of the solvent, porous PMMA nanostructures are obtained, reflecting the solvent-rich and polymer-rich phases.

The coarsening process of the solvent-rich phases in the PMMA/THF solution is studied by changing the immersion time, the polymer concentration, and the polymer molecular weight. Under conditions in which polymer solutions have higher viscosities, the coarsening process is slowed and the formation of porous nanostructures can be prohibited. The prevention of porous nanostructure formation can also be achieved by adding water to the PMMA/THF solution before the immersion process.

The phase-separation behavior of a polymer solution in cylindrical channels is different from that in other unconfined systems and provides a new way to prepare 1D porous nanostructures. The proposed coarsening model of the phase-separation process also has important implications for the operation and design of novel polymer nanomaterials using templates. For possible future work, we would like to apply the phase-separation concept to other functional materials such as silica, titania, and conjugated polymers. For example, blends of polymer and inorganic precursors can be used, and 1D porous inorganic nanomaterials might be fabricated.

ASSOCIATED CONTENT

Supporting Information

SEM images of AAO templates and PMMA nanostructures prepared under different conditions. This material is available free of charge via the Internet at http://pubs.acs.org.

AUTHOR INFORMATION

Corresponding Author

*E-mail: jtchen@mail.nctu.edu.tw. Tel: 886-3-5731631.

Notes

The authors declare no competing financial interest.

ACKNOWLEDGMENTS

This work was supported by the National Science Council.

REFERENCES

(1) Tran, H. D.; Li, D.; Kaner, R. B. One-Dimensional Conducting Polymer Nanostructures: Bulk Synthesis and Applications. *Adv. Mater.* **2009**, *21*, 1487−1499.

(2) Aleshin, A. N. Polymer Nanofibers and Nanotubes: Charge Transport and Device Applications. *Adv. Mater.* **2006**, *18*, 17−27.

(3) Lu, X. F.; Zhang, W. J.; Wang, C.; Wen, T. C.; Wei, Y. One-Dimensional Conducting Polymer Nanocomposites: Synthesis, Properties and Applications. *Prog. Polym. Sci.* **2011**, *36*, 671−712.

(4) Chen, J. T.; Hsu, C. S. Conjugated Polymer Nanostructures for Organic Solar Cell Applications. *Polym. Chem.* **2011**, *2*, 2707−2722.

(5) Martin, C. R. Nanomaterials - A Membrane-Based Synthetic Approach. *Science* **1994**, *266*, 1961−1966.

(6) Haberkorn, N.; Lechmann, M. C.; Sohn, B. H.; Char, K.; Gutmann, J. S.; Theato, P. Templated Organic and Hybrid Materials for Optoelectronic Applications. *Macromol. Rapid Commun.* **2009**, *30*, 1146−1166.

(7) Martin, J.; Maiz, J.; Sacristan, J.; Mijangos, C. Tailored Polymer-Based Nanorods and Nanotubes by "Template Synthesis": From Preparation to Applications. *Polymer* **2012**, *53*, 1149−1166.

(8) Zhang, L.; Vidyasagar, A.; Lutkenhaus, J. L. Fabrication and Thermal Analysis of Layer-by-Layer Micro- and Nanotubes. *Curr. Opin. Colloid Interface Sci.* **2012**, *17*, 114−121.

(9) Masuda, H.; Fukuda, K. Ordered Metal Nanohole Arrays Made by a 2-Step Replication of Honeycomb Structures of Anodic Alumina. *Science* **1995**, *268*, 1466−1468.

(10) Li, A. P.; Muller, F.; Birner, A.; Nielsch, K.; Gosele, U. Hexagonal Pore Arrays with a 50−420 nm Interpore Distance Formed by Self-Organization in Anodic Alumina. *J. Appl. Phys.* **1998**, *84*, 6023−6026.

(11) Martin, J.; Mijangos, C. Tailored Polymer-Based Nanofibers and Nanotubes by Means of Different Infiltration Methods into Alumina Nanopores. *Langmuir* **2009**, *25*, 1181−1187.

(12) Steinhart, M.; Wendorff, J. H.; Greiner, A.; Wehrspohn, R. B.; Nielsch, K.; Schilling, J.; Choi, J.; Gosele, U. Polymer Nanotubes by Wetting of Ordered Porous Templates. *Science* **2002**, *296*, 1997−1997.

(13) Chen, J. T.; Chen, W. L.; Fan, P. W. Hierarchical Structures by Wetting Porous Templates with Electrospun Polymer Fibers. *ACS Macro Letters* **2012**, *1*, 41−46.

(14) Maiz, J.; Martin, J.; Mijangos, C. Confinement Effects on the Crystallization of Poly(ethylene oxide) Nanotubes. *Langmuir* **2012**, *28*, 12296−12303.

(15) Lee, C. W.; Wei, T. H.; Chang, C. W.; Chen, J. T. Effect of Nonsolvent on the Formation of Polymer Nanomaterials in the Nanopores of Anodic Aluminum Oxide Templates. *Macromol. Rapid Commun.* **2012**, *33*, 1381−1387.

(16) Wu, H.; Su, Z. H.; Takahara, A. Gradient Composition Distribution in Poly(2,6-dimethylphenylene oxide)/Polystyrene Blend Nanorods. *Soft Matter* **2011**, *7*, 1868−1873.

(17) Chen, J. T.; Lee, C. W.; Chi, M. H.; Yao, I. C. Solvent-Annealing-Induced Nanowetting in Templates: Towards Tailored Polymer Nanostructures. *Macromol. Rapid Commun.* **2013**, *34*, 348−354.

(18) Mei, S. L.; Feng, X. D.; Jin, Z. X. Polymer Nanofibers by Controllable Infiltration of Vapour Swollen Polymers into Cylindrical Nanopores. *Soft Matter* **2013**, *9*, 945−951.

(19) Cepak, V. M.; Martin, C. R. Preparation of Polymeric Micro- And Nanostructures Using a Template-Based Deposition Method. *Chem. Mater.* **1999**, *11*, 1363−1367.
(20) Schlitt, S.; Greiner, A.; Wendorff, J. H. Cylindrical Polymer Nanostructures by Solution Template Wetting. *Macromolecules* **2008**, *41*, 3228−3234.
(21) Feng, X. D.; Jin, Z. X. Spontaneous Formation of Nanoscale Polymer Spheres, Capsules, or Rods by Evaporation of Polymer Solutions in Cylindrical Alumina Nanopores. *Macromolecules* **2009**, *42*, 569−572.
(22) van de Witte, P.; Dijkstra, P. J.; van den Berg, J. W. A.; Feijen, J. Phase Separation Processes in Polymer Solutions in Relation to Membrane Formation. *J. Membr. Sci.* **1996**, *117*, 1−31.
(23) Voorhees, P. W. The Theory of Ostwald Ripening. *J. Stat. Phys.* **1985**, *38*, 231−252.
(24) Song, S. W.; Torkelson, J. M. Coarsening Effects on Microstructure Formation in Isopycnic Polymer Solutions and Membranes Produced via Thermally Induced Phase Separation. *Macromolecules* **1994**, *27*, 6389−6397.
(25) Siggia, E. D. Late Stages of Spinodal Decomposition in Binary Mixtures. *Phys. Rev. A* **1979**, *20*, 595−605.
(26) Chou, Y. C.; Goldburg, W. I. Phase Separation and Coalescence in Critically Quenched Isobutyric-Acid-Water and 2,6-Lutidine-Water Mixtures. *Phys. Rev. A* **1979**, *20*, 2105−2113.
(27) Kuwahara, N.; Kubota, K. Spinodal Decomposition in a Polymer Solution. *Phys. Rev. A* **1992**, *45*, 7385−7394.